A New RSS Fingerprinting-Based Location Discovery Method Under Sparse Reference Point Conditions

ANG LI[ID], JINGQI FU, AOLEI YANG, AND HUAMING SHEN

Department of Mechatronics Engineering and Automation, Shanghai University, Shanghai 200444, China

Corresponding author: Jingqi Fu (jqfu@staff.shu.edu.cn)

ABSTRACT With the increasing demand for indoor location-based services, the received signal strength fingerprinting-based localization algorithm has become a research focus due to its accuracy and low hardware requirements. However, how to achieve the accurate location discovery relies solely on the received signal strength under the sparse reference points condition, which is the main contribution of this paper. First, the Voronoi diagram is adopted to regionalize the positioning area and form a distributed signal propagation description, which can reduce the influence of environment interference. Second, aiming at the local motion tracking problem, a region-based location search model is constructed to achieve the initial position estimation and provide the motion model for the following optimization of location estimation. Third, in order to reduce the cumulative error caused by the environmental noise and the local optimum problem, the regularized particle filtering algorithm with map-correction is employed to implement the dynamic calibration of the particle updating equation. To verify the proposed algorithm, an indoor wireless experiment system is finally designed in this paper. The experiment results indicate that the proposed algorithm can increase the positioning accuracy by 28.2% compared with the fingerprinting-based localization algorithm when the RPs density is reduced to 0.2/ (0.5m*0.5m).

INDEX TERMS Batch gradient descent, indoor positioning, regularized particle filtering, sparse reference points condition, Voronoi diagram.

I. INTRODUCTION

With the rapid development of internet of things (IoT) in recent years, the location-based services (LBSs) has attracted much attention due to its wide applications in daily lives. Indoor environments such as underground shopping centers which contain the complex multi-path, the non-line-of-sight propagation and so on. So the global positioning system can hardly meet the indoor positioning requirements. Thus, the indoor localization system has become a hot research point [1]–[4]. The received signal strength (RSS), the ultra wideband, the radio frequency identification and the visible light based indoor positioning strategy are differentiated by the inference techniques such as the time of arrival, the time difference of arrival and the angle of arrival [5]–[7]. Among several branches of positioning technologies, RSSs can provide position information without additional hardware supports. However, the RSS is vulnerable to the environmental noise, the antenna orientation, and the multi-path reflection,

these interference will result in the poor positioning accuracy. Since existing positioning technologies have deficiencies respectively, the accurate positioning can hardly be achieved by an individual method. The fingerprinting-based localization algorithm has drawn widespread attention for its high positioning accuracy [8].

The fingerprinting-based localization algorithm mainly includes two phases: 1) the establishment of offline reference point fingerprint (RPF) database; 2) the online fingerprint matching phase. In the offline phase, the RSS obtained from various beacon points (BPs) at each reference point (RP) can be described as RPF. The coordinate of RP and the received RPF can form a location-relevant database called RPF database. The location estimation can be obtained by matching the online RSS observation with the offline RPF database, this location discovery method is called as the fingerprinting-based localization algorithm. The accuracy of the fingerprinting-based indoor location tracking system is

mainly influenced by three aspects including the establishment/maintenance of RPF database, the fingerprint matching method and the cumulative positioning error.

A. THE ESTABLISHMENT/MAINTENANCE OF RPF DATABASE

In recent years, the channel state information (CSI) is used as the fingerprint in some study which is proved to be more stable and have more features to choose from [9]. In order to achieve the accurate positioning, the features of CSI would be extracted [10] and delivered to the processing unit to train the classifiers [11]. However, CSI fingerprints are also sensitive to the positioning environment [12]. When the positioning environment changes, the parameter of model and classifier need to be re-trained [13] to maintain the accuracy. Thus, the RSS based fingerprinting which is visualized and easy to be compensated, is remaining to be an important method in the indoor positioning system. To reduce the quantity of the RPs, a new PF scheme [14] is proposed, which contains the single-hidden layer feed-forward network for distinguishing similar fingerprints. Reference [15] proposed a calibration zero-effort system based on the crowdsourcing of the training data and achieved the target tracking using the inertial sensors contained in the mobile devices. The Gradlent FingerprinTing [16] which leverages a more stable RSS gradient is proposed to avoid the laborious of fingerprint map calibration. Reference [17] proposed a WiFi-based non-intrusive online radio map construction method, the proposed WinIPS can capture data packets and extract the RSS and MAC addresses from both WiFi access points and mobile devices in a non-intrusive manner. So, the WiFi access points can serve as online reference points and achieve the calibration-free indoor localization. A kernel-based learning technique [18] is proposed to increase the classification ability of fingerprint. In order to obtain appropriate fingerprint databases at different time phases, a mobile data-collection cart and a method to construct the time-relevant fingerprint database [19] are proposed. In [20], a Wi-Fi based indoor localization method is proposed to adopt assistant nodes with similar RSS sequences as auxiliary nodes to implement the accurate positioning in the complex indoor environment. In [21]–[23], fingerprints can be constructed based on the Voronoi diagram according to the signal propagation model [24], [25] and the signal attenuation parameter [26]–[28]. In a word, these methods could be used to decrease the reliance on the accuracy of the established RPF database. However, the study on the RPF database under the condition of sparse RPs are relatively rare.

B. FINGERPRINT MATCHING ALGORITHM

A novel likelihood estimation and a stochastic gradient descent location discovery algorithm [29] are proposed to deal with the inadequate received fingerprints. Reference [30] proposed a robust, cost-effective and scalable localization system to achieve the automatical search of model parameters through the training phase and improve the online matching accuracy. In [31], an improved image-based pedestrian

trajectory estimation method is proposed to use detected images as assistants. In [32] and [33], the indoor location tracking system equipped with measurement units such as the gyroscope, the step frequency and step length detection is proposed. Auxiliary measurement units are adopted to calibrate positioning-related parameters and improve the positioning and location tracking accuracy. However, these would increase the system construction complexity. Moreover, the positioning performance have not been verified under insufficient RP conditions.

C. DYNAMIC CUMULATIVE POSITIONING ERROR

The RPF database construction method is proposed in [34] and [35], which adopts the filtering algorithm to construct the real-time RPF database and compensate the cumulative positioning error. In [36], a location tracking algorithm is presented by using CAD floor plan as the constraint map. A virtual track (VT) location tracking method [37] is put forward when the map is hard to obtain, and the link trigger sequence is adopted to achieve the location discovery. The pedestrian dead reckoning (PDR) incorporated with the magnetometer technology is employed in [6] to reduce the cumulative positioning error through the azimuth map-correction mechanism. These studies indicate that the cumulative error can be weakened by the calibration maps, and the key bottleneck is the acquisition of accurate calibration map. To get the calibration map, every RP in the positioning area should be arranged to collect corresponding RPF samples constantly, which is a laborious and unpractical work. On the other hand, if the number of the deployed RP is decreased, the positioning accuracy can not be guaranteed by the above mentioned methods.

Under the same indoor positioning circumstance, the accuracy of the fingerprinting-based localization algorithm is related to on the RPF database, the more preset RPs, the more accurate positioning results. However, this is a labor-intensive and time-consuming process. The RP reduction incurs the degradation of the support information for establishing the RPF database, and it further results in the deterioration of the positioning performance. Therefore, it is an essential problem to achieve the accurate localization under the sparse RPs condition. Aiming at this problem, there are three aspects to be studied respectively: 1) how to truly reflect the propagation environment of local signals; 2) how to transform the indoor localization problem into the local optimization problem; 3) how to reduce the positioning accumulation error which is generated by environmental disturbances and local optimum problems.

The main contributions of this paper are summarized below.

1) A regionalization method for indoor environment is proposed based on preset RPs.

The Voronoi diagram is adopted to regionalize the positioning area into several Voronoi units based on preset RPs, and the signal attenuation parameter of each RP can represent the signal propagation characteristic of the entire Voronoi unit.

Thus, these environment-relevant Voronoi units can achieve a true reflection of the local signal propagation.

2) A location search model is constructed based on the proposed batch gradient descent (BGD) method with region-adaptive parameters.

The local searching algorithm integrated with the propagation parameter of Voronoi unit would achieve the adaptive construction of location search model. According to this model, the BGD algorithm can be applied to obtain an initial estimation of the mobile terminal (MT).

3) A regularized particle filtering algorithm with map-correction (MAPF) is proposed.

The movement model of the MT would be used as the particle updating equation in the regularized particle filtering algorithm. In order to reduce the cumulative positioning error timely, this paper proposes a map-correction mechanism for the displacement and azimuth estimation to modify the movement model. The movement of state particles can be corrected through the model modification, so the cumulative positioning error generated in the iteration can be prevented.

In order to verify the effectiveness of the proposed algorithm, some experimental configurations with different number of RPs are established respectively. Contrast experiments are conducted under different configurations and all experimental results in this paper were obtained in a chosen laboratory.

The rest of this paper is organized as follows. Section II proposes three solutions corresponding to three proposed key problems. The RPs based regionalization method for indoor environment, the location search model based on the proposed region-adaptive BGD method, and the MAPF algorithm are constructed and depicted in detail. In Section III, an indoor localization system is established and several experimental results are presented to verify the proposed algorithm.

II. APPROACH

The proposed indoor positioning algorithm is designed based on the fingerprinting-based localization algorithm and includes three aspects: the offline RPF database establishment, the online region-adaptive BGD location search, and the regularized particle filtering with map-correction.

As shown in Fig. 1, the only input of the proposed algorithm is the RSS fingerprint received from BPs. In the online matching phase, the received RSS fingerprint is compared with the regionalized RPF database to obtain the first matching RP and the corresponding Voronoi unit. Then, a location search algorithm based on the proposed region-adaptive BGD method is adopted to obtain the initial location estimation. Finally, the MAPF algorithm employ the proposed map-correction mechanism to calibrate the movement of state particles. In which, the movement model and Voronoi units are adopted as the map to correct the state particle updating equation and optimize the location estimation.
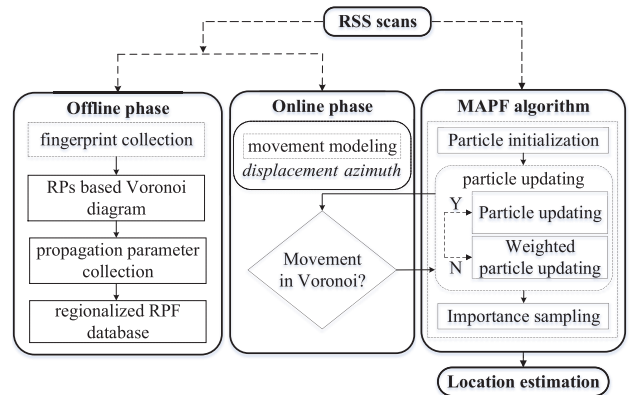

FIGURE 1. Indoor localization algorithm under sparse RPs condition.

A. PRE-SET RP BASED REGIONALIZATION METHOD FOR INDOOR ENVIRONMENT

The complex indoor positioning environment, including the furniture, the wall, the widely used electronic equipment etc., can cause the non-line-of-sight and the multi-path propagation interference on the signal propagation path. These will break the relationship between the propagation distance and the received RSS, and affect the positioning accuracy of the range-based method. Thus, the fingerprinting-based localization algorithm has attracted a lot of attentions since it can guarantee the high positioning accuracy without additional hardware support. This non-range-based algorithm mainly includes the offline RPF database acquisition phase and the online matching phase. Fig. 2 shows the algorithm structure.
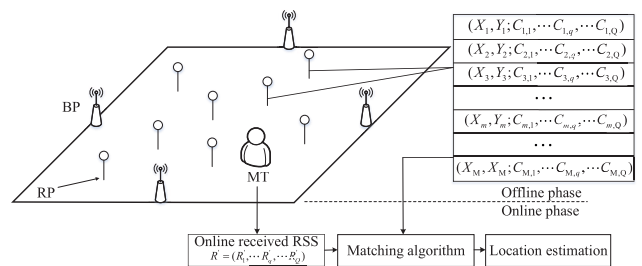

FIGURE 2. The structure of fingerprinting-based localization algorithm.

In Fig. 2, assuming that there are Q BPs, M RPs and one MT in the positioning area. In the offline RPF database establishment phase, BPs are fixed in the positioning area, and broadcast beacons according to a certain period. The MT carried by tester is located at the coordinate of the preset RP and receives beacons from all the BPs. The RSS extracted from received beacons are recorded as the fingerprint of the RP, and stored with RP coordinates to form the RPF database, which is given in (1),

$$(\underbrace{X_m, Y_m}_{coordinate} ; \underbrace{C_{m,1}, \cdots, C_{m,q}, \cdots, C_{m,Q}}_{RSS})$$

$$m \in [1, M], \quad q \in [1, Q] \quad (1)$$

$C_{m,q}$ denotes the RSS received from the qth BP at (X_m, Y_m), where (X_m, Y_m) denotes the coordinate of the mth RP. In the

online matching phase, the MT receives the real-time RSS from BPs, which is given in (2),

$$R' = (R'_1, R'_2, \cdots, R'_q, \cdots, R'_Q), \quad q \in [1, Q] \quad (2)$$

where, R'_q denotes the real-time RSS received from the qth BP. So R' denotes the integrated RSS fingerprint received from all BPs. The fingerprinting-based algorithm can obtain the most matching RPF by comparing R' with the RPF database. Then, the coordinate of the matched RPF is considered as the location estimation of the MT. The more RPs, the more accurate estimation. In order to acquire adequate RPs and complete the RPF database, assuming that the fingerprint should be collected for L times to guarantee the accuracy at one RP, so the establishment of the RPF database requires M*Q*L times fingerprint collection. This is a time-consuming work and would hinder the practical application of the indoor localization. Moreover, the signal propagation environment changes along with the movement of included objects, which results in the additional fingerprint calibration work. Therefore, the establishment and maintenance of the RPF database is a labor-intensive and time-consuming process.

The main problem of insufficient RPs is that the density of RPs can no longer match the positioning request. Several positioning results would occur at the same RP and decrease the localization accuracy. In order to achieve the accurate positioning under the insufficient RPs condition. The signal attenuation parameter is introduced into the fingerprinting localization algorithm to represent the local signal propagation condition, and find a more precise location than the matching reference point through the optimization algorithm. The signal attenuation parameter n, which denotes the indoor signal propagation environment, is not equal in different places. Thus, assuming a uniform attenuation parameter in the whole positioning area is not an effective method. In order to achieve the accurate positioning, the precise reflection of the signal propagation environment in the positioning area is an important task. Aiming at this problem, a preset RPs based regionalization method for the indoor environment is proposed in this paper. The positioning area can be regionalized into several Voronoi units based on RPs through the Voronoi diagram, then the signal propagation parameter n of the RP would be adopted to represent the signal propagation environment of the whole Voronoi unit.

In Fig.3, a plane is divided into several convex polygons by the Delaunay triangulation algorithm based on RPs (which are recognized as Voronoi cores). The dotted lines denote the
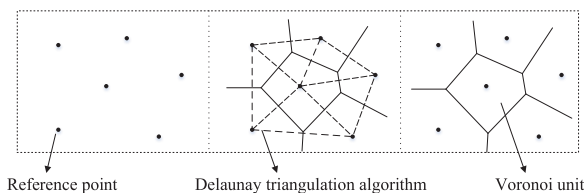

FIGURE 3. The construction method of Voronoi unit.

connection lines of RPs. The solid lines denote the vertical bisector of connection lines. The irregular convex polygons composed by solid lines are Voronoi units. According to the characteristic of Voronoi diagram, the Euclidean distance of the point inside Voronoi units to the inside RPs, are smaller than the distance to any other RPs, as shown in Fig.4.
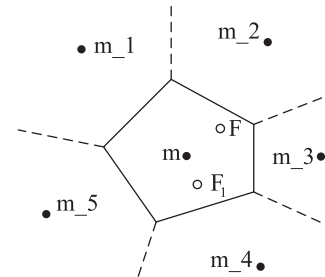

FIGURE 4. The diagram of Voronoi unit.

A case in point, $\{m, m\_1, m\_2, \cdots, m\_5\}$ denote a set of RPs labels. F is one location of the MT which is inside the mth Voronoi unit. The variable $d(F, m)$ denotes the distance between the mth BP and F, which is smaller than the distance between other RPs and F, the equation can be expressed by $d(F, m) < min\{d(F, m\_1), d(F, m\_2), \cdots, d(F, m\_5)\}$. Moreover, reference [20] proves that the geographically adjacent nodes have similar signal propagation conditions, that is, m and F have similar signal propagation conditions. Thus, m and F would receive similar fingerprints from BPs.

Inference 1: If the RSS received by the MT is similar with the recorded fingerprint of the mth RP, the signal propagation condition of the MT is similar to the mth RP. Thus, the coordinate of the MT is closest to the coordinate of the mth RP. (Assuming that the RPF database establishment and the online RSS reception of MT are under the same environment)

Similarly, F_1 inside the mth Voronoi unit would also satisfy $d(F_1, m) < min\{d(F_1, m\_1), \cdots, d(F_1, m\_5)\}$. That is, the signal propagation environment at point F and F_1 can be represented by parameter n of the mth RP.

Inference 2: The signal propagation environment at any position inside the Voronoi unit can be represented by the parameter n of the inside RP.

Thus, in order to achieve the precise reflection of the signal propagation environment, the parameter n of the Voronoi unit would be added to the RPF database and form the regionalized RPF database, which is given in (3),

$$(\underbrace{X_m, Y_m}_{coordinate}; \underbrace{C_{m,1}, \cdots, C_{m,Q}}_{RSS} | \underbrace{n_{m,1}, \cdots, n_{m,q}, \cdots, n_{m,Q}}_{propagation-index}),$$
$$m \in [1, M], q \in [1, Q] \quad (3)$$

where $n_{m,q}$ denotes the propagation parameter of signal propagation path, which can represent the strength attenuation degree from the qth BP to the mth RP. A RP has Q number of signal propagation parameters because there are Q number of BPs serving as signal emitters. Thereby, the regionalized RPF database that can implement the accurate reflection of the signal propagation environment is established.

Remark 1: The preset RPs based regionalization method for indoor environment mainly rely on RPs and the Voronoi diagram, the indoor positioning environment can be divided into several environment-related Voronoi units reasonably. Therefore, when the RPs are insufficient, an accurate regionalized RPF database can also be obtained through this method.

B. LOCATION SEARCH MODEL BASED ON THE PROPOSED REGION-ADAPTIVE BGD METHOD

After the reception of the real-time RSS fingerprint in the online phase, the location estimation of the MT can be obtained through the fingerprinting-based localization algorithm. However, when the preset RP is insufficient, there are not enough RPF for the fingerprint matching process. It is necessary to search a more accurate location around the first matched m^{th} RP. Therefore, the indoor positioning problem should be transformed into a local location search problem.

Shadowing model is a kind of signal attenuation model which is widely used in the RSS range-based algorithm. The RSS received at d meters away from the signal transmitter follows (4),

$$R = R_0 - 10n_{m,q}lg(\frac{d}{d_0}) + x_\sigma \qquad (4)$$

where, R_0 denotes the RSS received at the reference distance d_0 away from the signal transmitter. Generally, the reference distance d_0 is set to 1m. R denotes the RSS received at d meters away from the signal transmitter. Assuming that the process interference x_σ follows a normal distribution $N(0, \sigma^2)$. After the jth positioning request is sent, the MT receives beacons from all BPs. The RSS frame segment can be extracted from the received beacons and form a real-time fingerprint R_j, as given in (5),

$$R_j = (R_{j,1}, R_{j,2}, \cdots, R_{j,q}, \cdots, R_{j,Q}), q \in [1, Q] \qquad (5)$$

where, $R_{j,q}$ is the real-time RSS received from the qth BP during the jth positioning. Firstly, the most matched RP would be selected through the fingerprinting-based localization algorithm. The matching equation can be expressed as (6),

$$min(\frac{1}{Q}\sum_{q \in Q}|R_{j,q} - C_{m,q}|) \qquad (6)$$

In the sparse RP condition, the coordinate of the matched m^{th} can not be adopted as the location estimation because of the biases. The local location search problem is mainly to find a position surrounded the matched m^{th} voronoi core, where it can receive the most similar fingerprint compared with the real-time RSS. Assuming that $\tilde{R}_{j,q}$ is the RSS received from the qth BP at the location S_j, and the location S_j is inside the mth voronoi unite. According to (6), the objective function H can be defined as the average difference between $R_{j,q}$ and $\tilde{R}_{j,q}$, expressed by (7),

$$H = \frac{1}{Q}\sum_{q \in Q}|R_{j,q} - \tilde{R}_{j,q}| \qquad (7)$$

According to the **Inference 2**, the signal propagation condition of S_j can be represented by the $n_{m,q}$ of the mth Voronoi core. So, based on (4), $\tilde{R}_{j,q}$ can be expressed by (8),

$$\tilde{R}_{j,q} = R_0 - 10n_{m,q}lg(d(S_j, B_q)) \qquad (8)$$

where B_q denotes the coordinate of the qth BP, assuming that $S_j = (x_j, y_j)$, $B_q = (X_q, Y_q)$. So the distance between S_j and B_q can be described as $d(S_j, B_q) = \sqrt{(x_j - X_q)^2 + (y_j - Y_q)^2}$,

Thus, the objective function H can be expressed as (9),

$$H = \frac{1}{Q}\sum_{q \in Q}|R_{j,q} - R_0 + 10n_{m,q}lg(d(S_j, B_q))| \qquad (9)$$

According to (7), the objective is to search for a S_j which can minimize the objective function H, as given in the (10),

$$min(H) = min(\frac{1}{Q}\sum_{q \in Q}|R_{j,q} - R_0 + 10n_{m,q}lg(d(S_j, B_q))|) \qquad (10)$$

To minimize the objective function H, there exists some intelligent optimization methods including the particle swarm optimization (PSO), the simulated annealing (SA) and the genetic algorithm (GA) etc. The gradient descent algorithm possess the lower algorithm complexity than the intelligent optimization method and can be designed to various transformations for different application fields [38]. In this paper, after the segmentation of the positioning area based on the proposed regionalization method, each regionalized unit has an exclusive signal attenuation characteristic. So the regionalized unit can be incorporated with the gradient descent algorithm to find S_j efficiently. Moreover, there are some fixed BPs deployed in the established indoor positioning system, the direction towards each BP represents one orientation of the signal attenuation. According the mechanism of BGD, the BGD method can search for one synthesized direction based on these directions in time.

Based on the BGD algorithm, the opposite direction of the gradient is the fastest direction to decline for the objective function. Since the target is to minimize the objective function H, the search direction can be set to the opposite direction of the gradient.

1) If $R_0 - 10n_{m,q}\lg(\sqrt{(x_j - X_q)^2 + (y_j - Y_q)^2}) < R_{j,q}$, the objective function H can be expressed as (11),

$$H = \frac{1}{Q}\sum_{q \in Q}(R_{j,q} - R_0 + 10n_{m,q}lg(\sqrt{(x_j - X_q)^2 + (y_j - Y_q)^2}) \qquad (11)$$

The gradient of H can be expressed by (12),

$$grad(H) = (\frac{\partial H}{\partial x_j}, \frac{\partial H}{\partial y_j})$$

$$= (\frac{10}{Q\ln 10}\sum_{q \in Q}\frac{n_{m,q}(x_j - X_q)}{(x_j - X_q)^2 + (y_j - Y_q)^2},$$

$$\frac{10}{Q\ln 10}\sum_{q \in Q}\frac{n_{m,q}(y_j - Y_q)}{(x_j - X_q)^2 + (y_j - Y_q)^2}) \qquad (12)$$

Assuming that the step size is set to α, and the current position of MT S_j can be calculated through (13) according to the BGD algorithm,

$$
\begin{aligned}
S_j &= S_{j-1} - \alpha \cdot grad(H) \\
&= (x_{j-1} - \alpha \frac{\partial H}{\partial x_j}, y_{j-1} - \alpha \frac{\partial H}{\partial y_j}) \\
&= (x_{j-1} - \frac{10\alpha}{Q \ln 10} \sum_{q \in Q} \frac{n_{m,q}(x_j - X_q)}{(x_j - X_q)^2 + (y_j - Y_q)^2}, \\
&\quad y_{j-1} - \frac{10\alpha}{Q \ln 10} \sum_{q \in Q} \frac{n_{m,q}(y_j - Y_q)}{(x_j - X_q)^2 + (y_j - Y_q)^2})
\end{aligned} \quad (13)
$$

2) If $R_0 - 10n_{m,q} \lg(\sqrt{(x_j - X_q)^2 + (y_j - Y_q)^2}) > R_{j,q}$, the objective function H can be expressed as (14),

$$
H = -\frac{1}{Q} \sum_{q \in Q} (R_{j,q} - R_0 + 10n_{m,q} lg(\sqrt{(x_j - X_q)^2 + (y_j - Y_q)^2})) \quad (14)
$$

The gradient of H can be expressed by (15),

$$
\begin{aligned}
grad(H) &= (\frac{\partial H}{\partial x_j}, \frac{\partial H}{\partial y_j}) \\
&= (-\frac{10}{Q \ln 10} \sum_{q \in Q} \frac{n_{m,q}(x_j - X_q)}{(x_j - X_q)^2 + (y_j - Y_q)^2}, \\
&\quad -\frac{10}{Q \ln 10} \sum_{q \in Q} \frac{n_{m,q}(y_j - Y_q)}{(x_j - X_q)^2 + (y_j - Y_q)^2}) \quad (15)
\end{aligned}
$$

Assuming that the step size is set to α, and the current position of MT S_j can be calculated through (16) according to the BGD algorithm,

$$
\begin{aligned}
S_j &= S_{j-1} - \alpha \cdot grad(H) \\
&= (x_{j-1} - \alpha \frac{\partial H}{\partial x_j}, y_{j-1} - \alpha \frac{\partial H}{\partial y_j}) \\
&= (x_{j-1} + \frac{10\alpha}{Q \ln 10} \sum_{q \in Q} \frac{n_{m,q}(x_j - X_q)}{(x_j - X_q)^2 + (y_j - Y_q)^2}, \\
&\quad y_{j-1} + \frac{10\alpha}{Q \ln 10} \sum_{q \in Q} \frac{n_{m,q}(y_j - Y_q)}{(x_j - X_q)^2 + (y_j - Y_q)^2}) \quad (16)
\end{aligned}
$$

In the (13) (16), $n_{m,q}$ is the region-adaptive parameter which is recorded in the proposed regionalized RPF database at the offline phase. The region-adaptive BGD location search model (13)(16) is proposed based on the environment parameter $n_{m,q}$.

According to the change of the signal propagation environment, the location search model would change automatically to improve the search accuracy. Therefore, the local location search algorithm can be expressed by the pseudocode, shown as Algorithm 1.

Remark 2: The proposed algorithm can be used to establish the region-adaptive location search model through the variable parameter $n_{m,q}$ and improve the search accuracy. Thereby, the accurate and fast location search based on insufficient RPs has been achieved.

Algorithm 1 Regional Batch Gradient Descent

Input: $\alpha, S_{j-1}, R_{j,q}$
Output: S_j

1 **for** $j = 1, \cdots$ **do**
2   -Build the optimization function
3    $min(H) = \min(\frac{1}{Q} \sum_{q \in Q} |R_{j,q} - \tilde{R}_{j,q}|)$
4   -Find the gradient direction
5    $grad(H) = (\frac{\partial H}{\partial x_j}, \frac{\partial H}{\partial y_j})$
6   -Estimation of current location
7   **if** $R_0 - 10n_{m,q} \lg(\sqrt{(x_j - X_q)^2 + (y_j - Y_q)^2}) < R_{j,q}$
   then
8       $S_j = S_{j-1} - \alpha \cdot grad(H)$
      $= (x_{j-1} - \frac{10\alpha}{Q \ln 10} \sum_{q \in Q} \frac{n_{m,q}(x_j - X_q)}{(x_j - X_q)^2 + (y_j - Y_q)^2}, y_{j-1} -$
      $\frac{10\alpha}{Q \ln 10} \sum_{q \in Q} \frac{n_{m,q}(y_j - Y_q)}{(x_j - X_q)^2 + (y_j - Y_q)^2})$
9   **if** $R_0 - 10n_{m,q} \lg(\sqrt{(x_j - X_q)^2 + (y_j - Y_q)^2}) > R_{j,q}$
   then
10      $S_j = S_{j-1} - \alpha \cdot grad(H)$
      $= (x_{j-1} + \frac{10\alpha}{Q \ln 10} \sum_{q \in Q} \frac{n_{m,q}(x_j - X_q)}{(x_j - X_q)^2 + (y_j - Y_q)^2}, y_{j-1} +$
      $\frac{10\alpha}{Q \ln 10} \sum_{q \in Q} \frac{n_{m,q}(y_j - Y_q)}{(x_j - X_q)^2 + (y_j - Y_q)^2})$

C. REGULARIZED PARTICLE FILTERING WITH MAP-CORRECTION(MAPF)

In the process of the offline RPF database establishment and the online fingerprint matching, the signal interference would be inevitably involved. If the error caused by the interference cannot be corrected in time, the generated cumulative positioning error would affect the location estimation accuracy in the iteration. The particle filtering (PF) [39] algorithm is a state-equation-based method which has been proved to be suitable for solving the nonlinear filtering problem. The filtered result of the PF algorithm can be expressed by (17),

$$
E[f(x_j)] \approx \sum_{i=1}^{I} \tilde{W}_i(x_j^{(i)}) f(x_j^{(i)}) \quad (17)
$$

where I denotes the number of state particles participated in the iteration, $\tilde{W}_i(x_j^{(i)})$ denotes the weight of the ith state particle, and $E[f(x_j)]$ denotes the filtered result of the PF algorithm. However, the PF algorithm could not solve the particle starvation problem generated in the particle resampling phase, which will incur biased estimations. The regularized particle filtering could be used to obtain state particles from the continuous approximation distribution, thus the diversity of state particles can be guaranteed. The optimal bandwidth of the Gaussian kernel in the regularized particle filtering can

be expressed by (18),

$$h_{opt} = [4/(\lambda + 2)]^{\frac{1}{\lambda+4}} I^{-\frac{1}{\lambda+4}} \quad (18)$$

where λ denotes the dimension of the state vector.

Moreover, for the problem of the local optimum caused by the region-adaptive BGD location search, the estimation error caused by the local optimum problem would accumulate in the iteration process and cannot be corrected by the regularized particle filtering. In response to this problem, a MAPF algorithm is proposed in this paper. The proposed regionalized RPF database is adopted as the calibration map to modify the positioning biases caused by the local optimum problem, and achieve the accurate and consecutive location tracking.

Assuming that the current position estimation is S_j, the historical position estimation is S_{j-1}, and the iteration equation of the displacement and azimuth can be expressed by (19),

$$azimuth : \Delta E_j = \angle(S_j - S_{j-1})$$
$$displacement : \Delta d = ||S_j - S_{j-1}||_2 \quad (19)$$

where, ΔE_j denotes the change of azimuth and Δd denotes the change of displacement during two positioning requests. When the MT moves along arbitrary direction in the 2D plane, according to the dead-reckoning, the location estimation can be derived in (20),

$$S_j = S_{j-1} + \begin{bmatrix} \cos \Delta E_j \\ \sin \Delta E_j \end{bmatrix} \Delta d + w_j \quad (20)$$

where w_j denotes the system noise.

Based on the PF algorithm, equation (20) can be adopted as the updating model in the updating phase of state particles, as shown in Fig. 5.
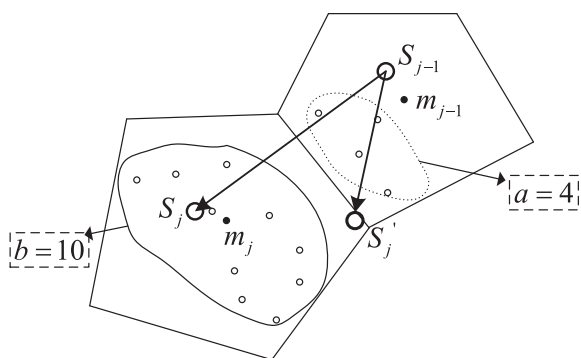

FIGURE 5. The schematic of map-correction mechanism.

The small circles refer to the state particles, and assuming these particles have been updated in the latest iteration. a denotes the number of particles in the historical m_{j-1}^{th} Voronoi unit. b denotes the number of particles in the current m_j^{th} Voronoi unit. If the real-time RSS contains too much ambient noise or the location search falls into a local optimum problem, the location estimation may appear at S_j'. It is necessary

to modify the updating equation and make the movement of particles to be closer to the real motion of the MT. Therefore, a weighted displacement and azimuth map-correction mechanism is proposed. Through the proposed map-correction mechanism, the location estimation can be optimized to S_j.

1) WEIGHTED AZIMUTH MAP-CORRECTION MECHANISM

a. If the chosen Voronoi unit of the current positioning gait S_j and the historical positioning gait S_{j-1} are the same, it indicates that the motion mainly occurs inside the chosen Voronoi unit. So, the azimuth deduced by (19) can be adopted without correction in (21),

$$\Delta \psi = \Delta E_j \quad (21)$$

b. If the chosen Voronoi unit of the current positioning gait S_j and the historical positioning gait S_{j-1} are different, it indicates that the signal propagation environment of these two estimation are different, so the deduced azimuth ΔE_j needs to be corrected. Assuming the reference azimuth among cores of the two chosen Voronoi unit is ΔV_j. The difference between ΔE_j and ΔV_j can be expressed by $\Delta \delta = |\angle(\Delta E_j, \Delta V_j)|$. If $\Delta \delta$ is large, it means the deduced azimuth of the particle movement deviates from the actual movement of the MT. So the weight of the reference azimuth ΔV_j needs to increase. Assuming $a_j = a/(a+b)$ denotes the number of state particles in the m_{j-1}^{th} Voronoi unit accounts for the proportion of all state particles, and $b_j = b/(a+b)$ denotes the number of state particles in the m_j^{th} Voronoi unit accounts for the proportion of all state particles. The azimuth map-correction mechanism can be expressed by (22),

$$\Delta \psi = \frac{a_j}{2} \Delta E_j (1 - \frac{\Delta \delta}{180°}) + \frac{b_j}{2} \Delta V_j (1 + \frac{\Delta \delta}{180°})$$
$$\Delta \delta = |\angle(\Delta E_j, \Delta V_j)|, \Delta \delta \in [0, 180°] \quad (22)$$

The updated particles distribution is adopted to implement the adaptive weight decision of reference azimuth ΔV_j and achieved the azimuth map-correction. If ΔE_j and ΔV_j are in the same quadrant, that means $\Delta \delta \in [0°, 90°)$, the corresponding weight of ΔE_j is $[0.5a_j, 0.25a_j)$, and ΔV_j is $[0.5b_j, 0.75b_j)$. If ΔE_j and ΔV_j are in different quadrants, the weight of ΔE_j is $[0.25a_j, 0]$, and the weight of ΔV_j is expressed as $[0.75b_j, b_j]$. As the difference $\Delta \delta$ between the deduced azimuth and the reference azimuth increases gradually, the weight of ΔE_j decreases from $0.5a_j$ to 0, and the weight of ΔV_j increases from $0.5b_j$ to b_j. This change indicates that if the azimuth estimation ΔE_j is close to the reference azimuth ΔV_j, the azimuth estimation will have more credibility.

Meanwhile, in order to integrate the azimuth map-correction mechanism, the symbol function $F = sgn(-|m_j - m_{j-1}|)$ can be constructed according to the relationship among the chosen Voronoi unit of adjacent positioning requests. Thus, the integrated azimuth map-correction

mechanism can be expressed by (23),

$$\Delta\psi = (1+F)\Delta E_j + (\frac{a_j}{2}\Delta E_j(1 + \frac{|\Delta E_j - \Delta V_j|}{180°}F))$$
$$+ \frac{b_j}{2}\Delta V_j(1 - \frac{|\Delta E_j - \Delta V_j|}{180°}F) \times (-F) \quad (23)$$

where, $\Delta\psi$ denotes the corrected azimuth estimation.

2) WEIGHTED DISPLACEMENT MAP-CORRECTION MECHANISM

Similarly, the weighted displacement map-correction mechanism is given in (24). The reference distance between the two chosen Voronoi unit cores $Distance(m_j, m_{j-1})$ is adopted to modify the displacement estimation.

$$\Delta D = \begin{cases} \Delta d_j, & m_j = m_{j-1} \\ a_j\Delta d_j + b_j Dis\tan ce(m_j, m_{j-1}), & m_j \neq m_{j-1} \end{cases} \quad (24)$$

where, ΔD is the corrected motion displacement.

When the two positioning are in the same Voronoi unit, the displacement estimation can be directly represented by Δd_j. If not the same, the displacement estimation is weighted corrected by the reference distance $Distance(m_j, m_{j-1})$.

Through these map-correction mechanism designed for state particle updating, the movement of state particles would be more similar to the actual motion of the MT. Thereby, the influence caused by the local optimum problem would be reduced in the iteration. The weighted displacement and azimuth map-correction mechanism can be expressed by the pseudocode, as shown in Algorithm 2.

Algorithm 2 Map-Correction Mechanism

---

1 **for** $i = 1 : I$ **do**

2    $x_j^i = x_{j-1}^i + \begin{bmatrix} \cos\Delta E_j \\ \sin\Delta E_j \end{bmatrix}\Delta d_j$

3   -Calculate the number of particles inside voronoi unit $(m_{j-1})^{th}$ a and inside voronoi unit $(m_j)^{th}$ b.

4   -Particle distribution weight:$a_j = \frac{a}{a+b}$, $b_j = \frac{b}{a+b}$

5   **if** $m_j = m_{j-1}$ **then**

6   -amendment function:

      $x_j^i = x_{j-1}^i + \begin{bmatrix} \cos\Delta E_j \\ \sin\Delta E_j \end{bmatrix}\Delta d_j$

7   **if** $m_j \neq m_{j-1}$ **then**

8      $\Delta\psi = \Delta(\frac{a_j}{2}\Delta E_j(1 - \frac{\Delta\delta}{180°}) + \frac{b_j}{2}\Delta V_j(1 + \frac{\Delta\delta}{180°}))$

     $\Delta D = a_j\Delta d_j + b_j Distance(m_j, m_{j-1})$

     -amendment function:

      $x_j^i = x_{j-1}^i + \begin{bmatrix} \cos\Delta\psi \\ \sin\Delta\psi \end{bmatrix}\Delta D$

9 †$Distance(m_j, m_{j-1})$ represents the Euclidean distance between m_j and m_{j-1}

Remark 3: The information of Voronoi unit and the regionalized RPF are integrated to design the map-correction mechanism and achieve the adaptively modification of the updating equation. Thus, the cumulative positioning error caused by

the environment interference and the local optimum problem can be prevented in the consecutive location tracking. In the case of insufficient RPs, the local and global movement estimation problem can be solved uniformly.

The MAPF algorithm can be expressed by the pseudocode, as shown in Algorithm 3.

III. EXPERIMENT RESULT
A. SYSTEM CONSTRUCTION

In order to verify the indoor positioning algorithm proposed in this paper, an indoor wireless localization system is constructed. The system mainly includes the gateway (G), the mobile measurement terminal (MT), beacon points (BP: B1, B2, B3, and B4), the PC and the processing software. The gateway is mainly responsible for receiving and storing the data received from each BP. The MT is carried by tester and provides RSS information to the gateway in time. The BP can provide its own physical coordinate, physical coordinates of the adjacent beacon point, and the RSS contained beacons. All of these information are packaged and transmitted to the PC through the gateway for the further processing. The main function of the PC and the processing software is to receive and store the measurement data from the gateway, and implement the indoor positioning algorithm proposed in this paper. Finally, the location estimation of the MT can be displayed on the user interface. The chips adopted as the gateway, the mobile measurement terminal and the beacon node are the CC2530 radio frequency chip based on the IEEE802.15.4 communication protocol produced by the TI Company. It works at the 2.4GHz frequency band and the transmission power is configured to +1dBm. The verification indoor positioning area is a floor containing a 5m*6m laboratory and a 6m*6m laboratory. The layout of the laboratory is shown in Fig. 6 (scene 1: one laboratory) and Fig. 12 (scene 2: two laboratory with a corridor). These are typical complex indoor environment which contains various staffs and devices.

In the 5m*6m laboratory (scene 1) shown in Fig. 6, four BPs (B1, B2, B3, and B4) are installed on the walls of the experiment laboratory respectively.

It can be deduced from the second section that the positioning accuracy is not only related to the number of RP, but also closely related to the node partitioning, the positioning environment, the positioning algorithm, etc. Therefore, it is difficult to find a critical condition about whether the environment is sparse. The method to decide the threshold of sparseness can refer to [23]. Under the same positioning environment, the RPs density, which is required by the fingerprint-based localization algorithm to achieve a certain accuracy, can be recorded as the threshold. If the density of RPs is less than the threshold density, the environment would be considered as sparse. According to this method, the sparse threshold in this paper is set to be 1.2/ (0.5m*0.5m), which is required by the fingerprinting-based localization to achieve the positioning error less than 0.5m. Five sparse conditions are configured

---

Algorithm 3 MAPF Algorithm

Input: $R_{j,q}$
Output: X_j

1 -Generate initial state particles: $\{x_1^i\}_{i=1}^I$
2 **for** $j = 1$ **do**
3   -Find the most matching fingerprint m_1
4   -Using region-adaptive BGD location search model to get location estimation S_j

5 **for** $j = 2, \cdots$ **do**
6   -find most matching fingerprint m_j
7   -Using R-EABGD method to get location estimation $S_j = S_{j-1} - \alpha \cdot grad(H)$
8   -State particle updating and evaluation phase
9   **for** $i = 1 : I$ **do**
10          $x_j^i = x_{j-1}^i + \begin{bmatrix} \cos \Delta E_j \\ \sin \Delta E_j \end{bmatrix} \Delta d_j$
11   -Map amendment mechanism:
12   **if** $m_j = m_{j-1}$ **then**
13   -amendment function:
                 $x_j^i = x_{j-1}^i + \begin{bmatrix} \cos \Delta E_j \\ \sin \Delta E_j \end{bmatrix} \Delta d_j$
14   **if** $m_j \neq m_{j-1}$ **then**
15              $\Delta \psi =$
                 $\Delta(\frac{a_j}{2} \Delta E_j(1 - \frac{\Delta \delta}{180°}) + \frac{b_j}{2} \Delta V_j(1 + \frac{\Delta \delta}{180°}))$
                 $\Delta D = a_j \Delta d_j + b_j Distance(m_j, m_{j-1})$
                 -amendment function:
                 $x_j^i = x_{j-1}^i + \begin{bmatrix} \cos \Delta \psi \\ \sin \Delta \psi \end{bmatrix} \Delta D$
16          $\widetilde{\omega}_j^i = \frac{1}{\sqrt{(2\pi)^4 \ det(R)}} exp\{-\frac{1}{2}(S_j - h_j(x_j^i))^T R^{-1}(S_j - h_j(x_j^i))\}$

17   -Calculate the sum of weights: $wsum = \sum_{i=1}^I \widetilde{\omega}_j^i$
         for $i = 1 : I$ **do**
18   Normalization: $\omega_j^i = wsum^{-1} \widetilde{\omega}_j^i$

19   -State particle resampling phase
20   Calculate the empirical covariance matrix var_{xy} of the sample set $\{\widehat{x}_j^i\}_{i=1}^I$.
21   Compute standard deviation sta_{xy}.
22   Initialize the cumulative sum of weights (CSW):$c_1 = \omega_j^1$.
23   **for** $i = 2 : I$ **do**
24          $c_i = c_{i-1} + \omega_j^i$
25      $u_1 \sim u[0, I^{-1}]$
26   **for** $s = 1 : I$ **do**
27          $u_s = u_1 + I^{-1}(s - 1)$
28   **while** $u_s > c_i$ **do**
29              $i = i + 1$
30          $x_j^{s*} = x_j^i$
31   **for** $i = 1 : I$ **do**
32   Draw$\epsilon^i \sim K$
33          $x_j^{i**} = x_j^{i*} + h_{opt} sta_{xy} \epsilon^i$
34      $X_j = I^{-1} \sum_{i=1}^I x_j^{i**}$

35 †R represents the covariance of measurement noise vector
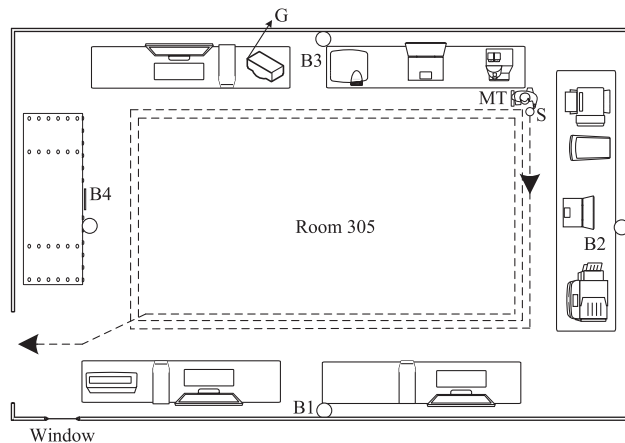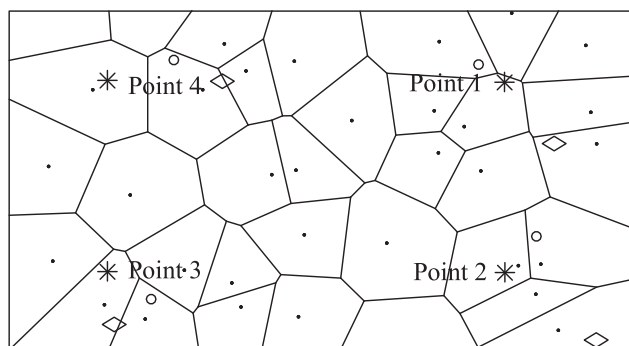

FIGURE 6. The schematic of positioning area.

FIGURE 7. Location estimation based on different database.

in scene 1 respectively, the RP densities are: 1 / (0.5m * 0.5m), 0.4 / (0.5m * 0.5m), 0.3 / (0.5m * 0.5m), 0.2 / (0.5m * 0.5m), 0.1 / (0.5m * 0.5m), the corresponding number of RPs are: 37, 15, 10, 7, and 5. Therefore, the proposed indoor localization algorithm can be verified under these configured sparse conditions.

B. EXPERIMENT RESULTS AND ANALYSIS
1) EXPERIMENT RESULTS AND ANALYSIS OF REGIONALIZED RPF DATABASE

When the number of RPs is 37, the location discovery algorithm is performed at four test points, based on the regular RPF database and the proposed regionalized RPF (R-RPF) database respectively. Fig. 7 shows the positioning results, and Table 1 shows the positioning error. In Fig.7, the star represents the true coordinates of the four test positions, the diamond represents location estimations using the RPF database with a uniform parameter n, and the circle represents location estimations using the R-RPF database.

In Fig. 7, the circle (estimations based on the R-RPF database) is closer to the star (position indications of the test position) than the diamond (estimations based on the RPF database). Table 1 shows the positioning error of the test point respectively, which indicates that the proposed regionalized RPF database can reflect the signal propagation environment

TABLE 1. Positioning error based on different database.

Chosen database	RPF database (m)	R-RPF database (m)
Point 1	0.58	0.19
Point 2	0.70	0.36
Point 3	0.39	0.38
Point 4	0.65	0.55

more accurately, thereby the better location estimation can be obtained.

2) LOCATION ESTIMATION AND ANALYSIS OF REGION-ADAPTIVE BGD LOCATION SEARCH MODEL

On the basis of the R-RPF database, in order to verify the location estimation performance of the region-adaptive BGD location search method proposed in this paper. 10 test points are selected in the positioning area, the MT is carried by the tester and passes the test points clockwise from the upper right point S, as shown in Fig. 6. When the number of RPs is 37, the location estimation performance of the proposed positioning algorithm is compared with the fingerprinting-based localization algorithm, as shown in Fig. 8.
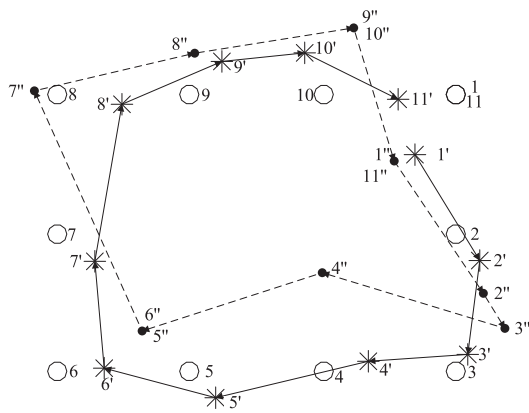

FIGURE 8. Comparison between PF algorithm and region-adaptive BGD algorithm.

As shown in Fig. 8, the circle denotes the true coordinates of test points, the solid line with stars denotes location tracking performance obtained by the region-adaptive BGD location search method proposed in this paper, and the dotted line denotes the location tracking results of the fingerprinting-based localization algorithm. The positioning results of the fingerprinting-based localization algorithm frequently located on the same RP under the insufficient RPs condition. However, the region-adaptive BGD location search method can still have good positioning performance.

### 3) EXPERIMENT RESULTS AND ANALYSIS OF MAPF

Since the environmental noise contained in the received RSS, and the local optimum problem caused by the BGD search method may influence the accuracy of the location estimation. These biases would be incorporated into the iteration

and cause a large cumulative positioning error if cannot be corrected in time. When the number of RPs is 37, aiming to the same 10 test point in Fig. 8, a group of location estimations which may suffer from the local optimum problem is shown in Fig. 9.
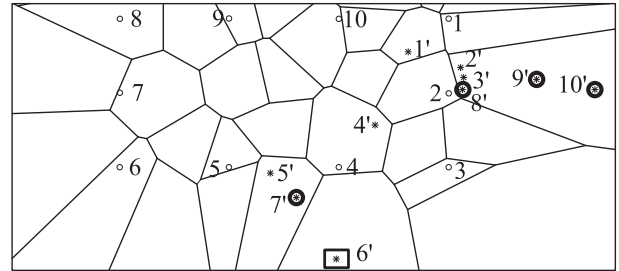
FIGURE 9. Positioning performance without map-correction.

In Fig. 9, the circle labeled 1-10 represent the real location of MT, and the star labeled 1'-10' denote the corresponding location estimation. In Fig. 9, the location estimations of the first five test points are close to the real location of them. In the sixth positioning, the location estimation contains a lot of bias compared with the real location due to the influence of the environmental noise or the local optimum problem. Then, this positioning error results in a more worse estimation at the following seventh test point and iteratively causes an increasing accumulated error. In order to intuitively describe the performance of the proposed MAPF algorithm, the positioning error comparison between the MAPF algorithm and the PF algorithm under the existence of the biased positioning is shown in Fig. 10.
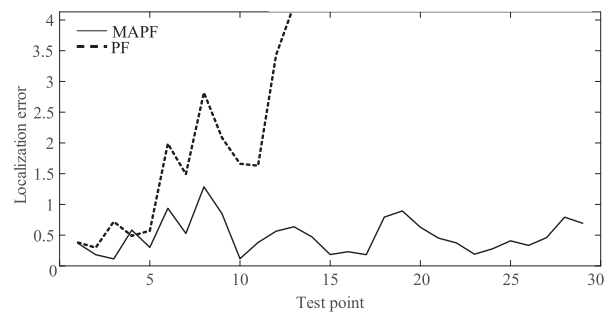
FIGURE 10. Comparison between MAPF algorithm and PF algorithm.

In Fig. 10, the dotted line denotes the positioning error of the PF algorithm. The error curve gradually expands after the appearance of the biased positioning at the sixth test point, which indicates that the accumulated errors cannot be corrected by the PF algorithm. The solid line represents the positioning error of the MAPF algorithm. It can be deduced from the curve, the positioning error can be restricted in a reasonable range through the map-correction mechanism performed in the seventh positioning. Thus, the robustness of the consecutive location tracking can be guaranteed.

4) EXPERIMENTAL RESULTS COMPARISON UNDER DIFFERENT RP SPARSENESS

In order to verify the performance of the proposed indoor localization algorithm under different degrees of insufficient RPs conditions, the MT is carried by the tester and moves clockwise along the trajectory from the point S, as shown in Fig. 6. Fig. 11 shows the recorded positioning results of the proposed indoor localization algorithm when the number of RPs is 15. The solid line with the star is the tracking results of the first cycle, the solid line with the triangle represents the second cycle, and the solid line with the four-pointed star represents the last half-cycle. It can be seen from Fig. 11 that the positioning results are basically consistent with the actual motion trajectory.
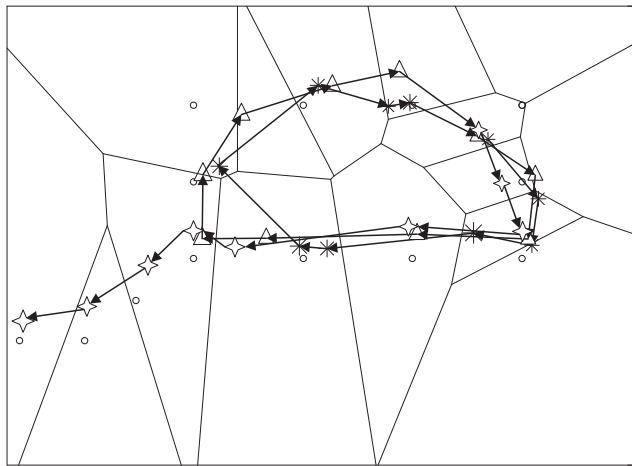

FIGURE 11. Location tracking results of proposed MAPF algorithm.

The Fig. 11 shows the location tracking performance of the proposed MAPF algorithm inside one laboratory. It is necessary to conduct the experiment in more expansive indoor environment. Thus, two adjacent laboratories in one floor (scene 2) are chosen as positioning area and the layout of the floor is depicted in Fig. 12.

There are nine BPs deployed in the positioning area. According to the chosen method of the reference points density, one RP sufficient condition and five RP sparse conditions are configured respectively, the corresponding number of RPs are: 87, 72, 28, 20, 14, 8.

The MT is carried by the tester and moves along the trajectory from the point S_f in Fig 12. There are 40 preset test points and 14 RPs deployed in the positioning area. The RP density is set to be 0.2 / (0.5m * 0.5m) which is the sparsest density that can maintain the positioning function in the experiments of room 305. Thus, the performance of the proposed algorithm would be verified in the new scene under the sparsest RP density firstly.

Fig. 13 shows the location tracking results of the proposed MAPF algorithm, the mean and min/max positioning error are presented in Table 2. According to the tracking trajectory, the proposed MAPF can achieve a good localization
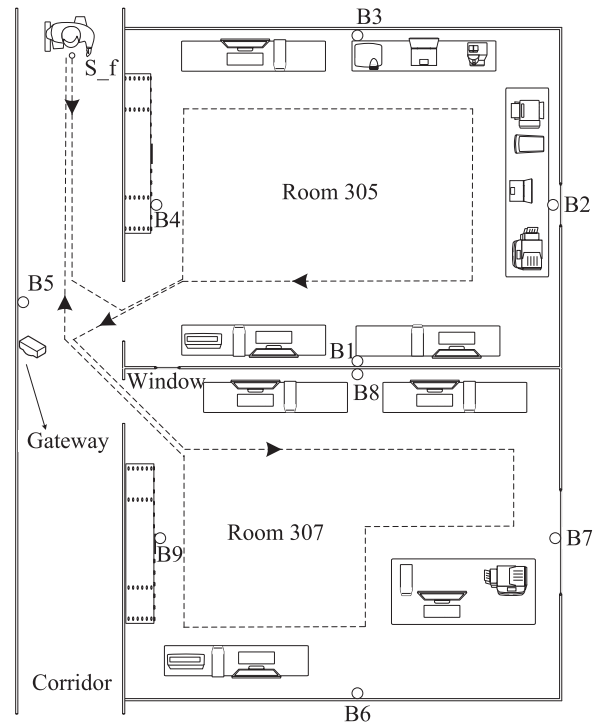

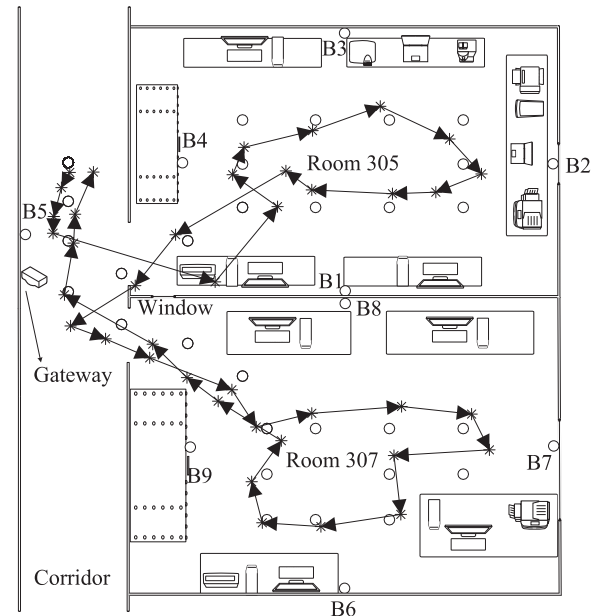**FIGURE 12.** Floor layout of the positioning area.

FIGURE 13. Localization results of the floor with multiple rooms.

TABLE 2. Localization results of one floor with multiple rooms.

	Average error	Max error	Min error
FL(m)	0.9225	2.3769	0.0255
MAPF(m)	0.6627	1.7847	0.0601

performance and improve the average positioning accuracy by 28.2% compared to the FL algorithm. The main problem of positioning under the insufficient RPs environment is that
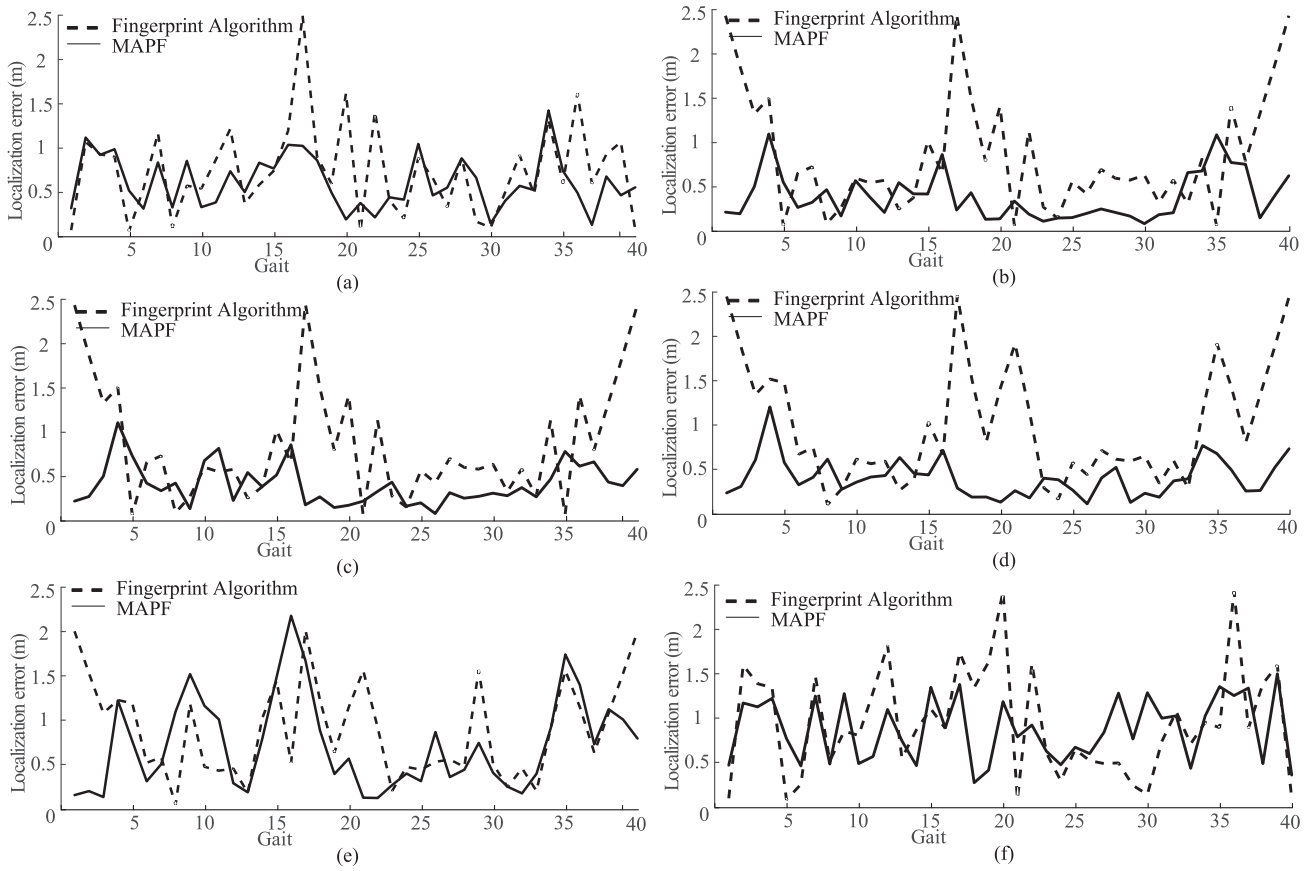
FIGURE 14. Comparison of positioning error under different RPs sparseness conditions. (a) 72 fingerprints. (b) 28 fingerprints. (c) 20 fingerprints. (d) 14 fingerprints. (e) 8 fingerprints. (f) 87 fingerprints.

the density of RPs is too low to supply enough location information for each step of the tester. However, the proposed MAPF algorithm can search for the more accurate location surround the sparse RPs, and decrease the max error from 2.3769m to 1.7847 m. These results proved that the proposed MAPF is suitable to positioning under insufficient RPs.

This experiment cost about 140 seconds with 40 test points under 14 RPs, which run on a computer with 3.2GHz AMD Ryzen 5 1600 CPU and 8 GB memory. The process time is relevant to the property of the processing unit, the RP density, the signal propagation condition and the termination of the location search algorithm.

In order to obtain the detailed positioning results of the MAPF algorithm under different RP densities, the experiment is conducted under six RP sparseness conditions respectively. The average, variance, and maximum of the positioning error are shown in Table 3 and Fig. 14.

Fig. 14 and Table 3 show that, under the sufficient RPs condition (with 87 RPs), the FL algorithm and the proposed algorithm can both achieve the good positioning performance. With the decrease of the RPs number, the performance of FL algorithm will deteriorate rapidly while the proposed MAPF algorithm can maintain the robust and accurate performance. When the number of RPs is reduced to 14, the average positioning error of the FL algorithm and the proposed

TABLE 3. Average positioning error under different RP sparseness conditions.

RP number	87	72	28	20	14	8
FL(m)	0.38	0.52	0.79	0.80	0.92	1.04
Variance(FL)	0.10	0.10	0.44	0.44	0.44	0.43
Max error(FL)	1.46	1.46	2.38	2.38	2.38	2.38
MAPF(m)	0.39	0.39	0.43	0.54	0.66	0.98
Variance(MAPF)	0.07	0.08	0.15	0.15	0.18	0.41
Max error(MAPF)	1.11	1.13	1.36	1.65	1.78	2.91

algorithm is 0.92m and 0.66m respectively. It can be deduced that, with the decrease of the RPs number, the proposed algorithm can increase the average positioning accuracy by 28.2% compared to the FL algorithm. When the number of RPs cannot support the positioning requests, the proposed MAPF algorithm would compensate and maintain the positioning accuracy.

As shown in Fig. 14(e), when the number of RPs drops to 8, the variance and the positioning error of the proposed MAPF drops to 0.41 and 0.98. It means that the positioning performance of the fingerprinting-based localization and the MAPF algorithm are both seriously deteriorated. This result indicates that the number of preset RPs cannot be less than 8 in the described indoor positioning environment, because the supplied information is too less to implement the positioning.
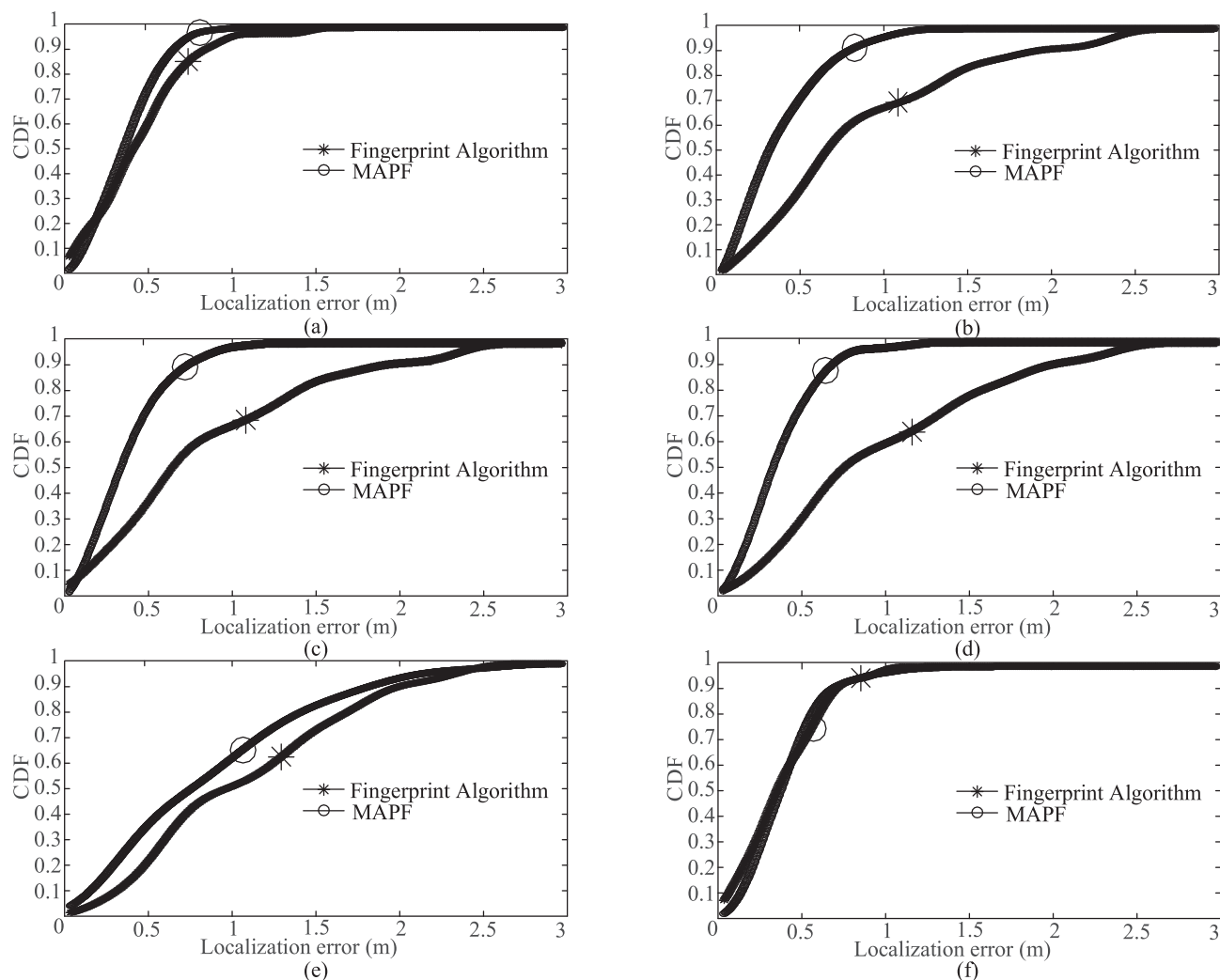
FIGURE 15. The CDF of consecutive positioning under different RPs sparseness conditions. (a) 72 fingerprints. (b) 28 fingerprints. (c) 20 fingerprints. (d) 14 fingerprints. (e) 8 fingerprints. (f) 87 fingerprints.

In order to verify the proposed indoor localization algorithm in the consecutive location tracking, the positioning experiments are carried out for 30 times under the six RP configurations. The cumulative distribution function (CDF) can be obtained as shown in Fig. 15.

In Fig. 15, the line with circle represents the CDF of the proposed algorithm and the line with star represents the CDF of the FL algorithm. As shown in Fig.15 (f), the probability of the positioning error within 1 meter are both above 95% based on these algorithms. The similar lines denote that both of the algorithm can achieve good performance when the number of RPs is sufficient. As shown in Fig. 15 (a)(b)(c)(d), the number of the preset RPs are set to be 72, 28, 20, 14 and form four RPs sparse conditions. The line with star is much lower than the line with circle, which denotes that the probability of the accurate positioning of the proposed algorithm is higher than the contrastive FL algorithm. Therefore, the proposed MAPF algorithm can achieve a good performance in the consecutive location tracking under RPs sparse condition.

TABLE 4. Probability of positioning error within 1 meter.

RP number	87	72	28	20	14
FL (%)	99.6	97.5	70.0	67.5	60.0
MAPF (%)	99.1	98.9	98.5	98.4	97.9

Moreover, as shown in Table 4, the Table 4 denotes the probability of the positioning error within 1 meter. When the number of RPs is reduced from 87 to 14, the probability of FL algorithm decreases from 99.6% to 60.0%. While, the proposed indoor localization algorithm can still remain above 95%. It indicates that, when the RPs density is reduced to 0.2/ (0.5m*0.5m), the probability of the proposed MAPF algorithm can be increased by 37.9% compared with the FL algorithm.

In summary, the proposed indoor localization algorithm can achieve the good positioning performance under the sparse RPs condition in the indoor scenes.

IV. CONCLUSION

This paper have proposed an optimization methods fused indoor positioning algorithm for the sparse RPs environment. There are three contributions have been made, including the establishment of the regionalized RPF database, the design of the region-adaptive location search model and the optimization method for the location estimation. The constructed verification system provides the convinced results under six configured conditions. For the proposed indoor localization algorithm, the localization accuracy can be increased by 28.2% under 0.2/ (0.5m*0.5m) RP density. The probability of the positioning error within 1 m can maintain 95% under the RPs density of 1.2-0.2/ (0.5m*0.5m), whereas the probability of the compared fingerprinting-based localization algorithm decrease rapidly to 60.0% with the decreasing density of RPs. In the indoor location based service, it is desirable to minimize the number of RPs while maintaining the positioning accuracy, which has been achieved by the proposed algorithm in this paper.

REFERENCES

[1] W. Ruan, Q. Z. Sheng, L. Yao, X. Li, N. J. G. Falkner, and L. Yang, "Device-free human localization and tracking with UHF passive RFID tags: A data-driven approach," *J. Netw. Comput. Appl.*, vol. 104, pp. 78–96, Feb. 2018, doi: 10.1016/j.jnca.2017.12.010.

[2] Q. Wang et al., "Light positioning: A high-accuracy visible light indoor positioning system based on attitude identification and propagation model," *Int. J. Distrib. Sensor Netw.*, vol. 14, no. 2, pp. 1–14, Feb. 2018, doi: 10.1177/1550147718758263.

[3] G. Caso, M. T. P. Le, L. De Nardis, and M.-G. Di Benedetto, "Performance comparison of WiFi and UWB fingerprinting indoor positioning systems," *Technologies*, vol. 6, no. 1, p. 14, Mar. 2018, doi: 10.3390/technologies6010014.

[4] D. Lymberopoulos, J. Liu, X. Yang, R. R. Choudhury, V. Handziski, and S. Sen, "A realistic evaluation and comparison of indoor location technologies: Experiences and lessons learned," in *Proc. 14th Int. Conf. Inf. Process. Sensor Netw.*, 2015, pp. 178–189.

[5] A. Yassin et al., "Recent advances in indoor localization: A survey on theoretical approaches and applications," *IEEE Commun. Surveys Tuts.*, vol. 19, no. 2, pp. 1327–1346, 2nd Quart., 2017, doi: 10.1109/COMST.2016.2632427.

[6] C. S. Wu, Z. Yang, and C. Xiao, "Automatic radio map adaptation for indoor localization using smartphones," *IEEE Trans. Mobile Comput.*, vol. 17, no. 3, pp. 517–528, Mar. 2018, doi: 10.1109/TMC.2017.2737004.

[7] J. Wang, P. Wang, and Z. Chen, "A novel qualitative motion model based probabilistic indoor global localization method," *Inf. Sci.*, vol. 429, pp. 284–295, Mar. 2018, doi: 10.1016/j.ins.2017.11.025.

[8] X. Tian, R. Shen, D. Liu, Y. Wen, and X. Wang, "Performance analysis of RSS fingerprinting based indoor localization," *IEEE Trans. Mobile Comput.*, vol. 16, no. 10, pp. 2847–2861, Oct. 2017, doi: 10.1109/TMC.2016.2645221.

[9] T. Li, H. Wang, Y. Shao, and Q. Niu, "Channel state information–based multi-level fingerprinting for indoor localization with deep learning," *Int. J. Distrib. Sensor Netw.*, vol. 14, no. 10, pp. 1–12, Oct. 2018, doi: 10.1177/1550147718806719.

[10] L. Zheng, B. Hu, and H. Chen, "A high accuracy time-reversal based WiFi indoor localization approach with a single antenna," *Sensors*, vol. 18, no. 10, p. 3437, Oct. 2018, doi: 10.3390/s18103437.

[11] Y. Wang, C. Xiu, X. Zhang, and D. Yang, "WiFi indoor localization with CSI fingerprinting-based random forest," *Sensors*, vol. 18, no. 9, p. 2869, Sep. 2018, doi: 10.3390/s18092869.

[12] J. Wang et al., "Low human-effort, device-free localization with fine-grained subcarrier information," *IEEE Trans. Mobile Comput.*, vol. 17, no. 11, pp. 2550–2563, Nov. 2018, doi: 10.1109/TMC.2018.2812746.

[13] J. Liu, L. Wang, J. Fang, L. Guo, B. Lu, and L. Shu, "Multi-target intense human motion analysis and detection using channel state information," *Sensor*, vol. 18, no. 10, p. 3379, Oct. 2018, doi: 10.3390/s18103379.

[14] Z. Wu, E. Jedari, R. Muscedere, and R. Rashidzadeh, "Improved particle filter based on WLAN RSSI fingerprinting and smart sensors for indoor localization," *Comput. Commun.*, vol. 83, pp. 64–71, Jun. 2016, doi: 10.1016/j.comcom.2016.03.001.

[15] R. Anshul, K. K. Chintalapudi, V. N. Chintalapudi, and R. Sen, "Zee: Zero-effort crowdsourcing for indoor localization," in *Proc. 18th Annu. Int. Conf. Mobile Comput. Netw.*, Istanbul, Turkey, 2012, pp. 293–304.

[16] Y. Shu et al., "Gradient-based fingerprinting for indoor localization and tracking," *IEEE Trans. Ind. Electron.*, vol. 63, no. 4, pp. 2424–2433, Apr. 2016, doi: 10.1109/TIE.2015.2509917.

[17] H. Zou, M. Jin, H. Jiang, L. Xie, and C. J. Spanos, "WinIPS: WiFi-based non-intrusive indoor positioning system with online radio map construction and adaptation," *IEEE Trans. Wireless Commun.*, vol. 16, no. 12, pp. 8118–8130, Dec. 2017, doi: 10.1109/TWC.2017.2757472.

[18] J. Yan L. Zhao, J. Tang, Y. Chen, R. Chen, and L. Chen, "Hybrid kernel based machine learning using received signal strength measurements for indoor localization," *IEEE Trans. Veh. Technol.*, vol. 67, no. 3, pp. 2824–2829, Mar. 2018, doi: 10.1109/TVT.2017.2774103.

[19] J. Zuo, S. Liu, H. Xia, and Y. Qiao, "Multi-phase fingerprint map based on interpolation for indoor localization using iBeacons," *IEEE Sensors J.*, vol. 18, no. 8, pp. 3351–3359, Apr. 2018, doi: 10.1109/JSEN.2018.2789431.

[20] Q. Li, W. Li, W. Sun, J. Li, and Z. Liu, "Fingerprint and assistant nodes based Wi-Fi localization in complex indoor environment," *IEEE Access*, vol. 4, pp. 2993–3004, 2016, doi: 10.1109/ACCESS.2016.2579879.

[21] J. Qin, S. Sun, Q. Deng, L. Liu, and Y. Tian, "Indoor trajectory tracking scheme based on delaunay triangulation and heuristic information in wireless sensor networks," *Sensors*, vol. 17, no. 6, p. 1275, Jun. 2017, doi: 10.3390/s17061275.

[22] Y. Wang, "Positioning locality using cognitive directions based on indoor landmark reference system," *Sensors*, vol. 18, no. 4, p. 1049, Apr. 2018, doi: 10.3390/s18041049.

[23] C. He, S. Guo, Y. Wu, and Y. Yang, "A novel radio map construction method to reduce collection effort for indoor localization," *Measurement*, vol. 94, pp. 423–431, Dec. 2016, doi: 10.1016/j.measurement.2016.08.021.

[24] J. M. Castro-Arvizu, J. Vilà-Valls, A. Moragrega, P. Closas, and J. A. Fernandez-Rubio, "Received signal strength–based indoor localization using a robust interacting multiple model–extended Kalman filter algorithm," *Int. J. Distrib. Sensor Netw.*, vol. 13, no. 8, pp. 1–16, Aug. 2017, doi: 10.1177/1550147717722158.

[25] R. K. Mahapatra and N. S. V. Shet, "Localization based on RSSI exploiting Gaussian and averaging filter in wireless sensor network," *Arabian J. Sci. Eng.*, vol. 43, no. 8, pp. 4145–4159, Aug. 2018, doi: 10.1007/s13369-017-2826-2.

[26] C. H. Tseng and J.-S. Yen, "Enhanced Gaussian mixture model of RSSI purification for indoor positioning," *J. Syst. Archit.*, vol. 81, pp. 1–6, Nov. 2017, doi: 10.1016/j.sysarc.2017.10.003.

[27] S. B. Shah et al., "3D weighted centroid algorithm & RSSI ranging model strategy for node localization in WSN based on smart devices," *Sustain. Cities Soc.*, vol. 39, pp. 298–308, May 2018, doi: 10.1016/j.scs.2018.02.022.

[28] K. Han, H. Xing, Z. Deng, and Y. Du, "A RSSI/PDR-based probabilistic position selection algorithm with NLOS identification for indoor localisation," *ISPRS Int. J. Geo-Inf.*, vol. 7, no. 6, p. 232, Jun. 2018, doi: 10.3390/ijgi7060232.

[29] K. Dong, Z. Ling, X. Xia, H. Ye, W. Wu, and M. Yang, "Dealing with insufficient location fingerprints in Wi-Fi based indoor location fingerprinting," *Wireless Commun. Mobile Comput.*, vol. 2017, Jun. 2017, Art. no. 1268515, doi: 10.1155/2017/1268515.

[30] T. Guan, L. Fang, W. Dong, D. Koutsonikolas, G. Challen, and C. Qiao, "Robust, cost-effective and scalable localization in large indoor areas," *Comput. Netw.*, vol. 120, pp. 43–55, Jun. 2017, doi: 10.1016/j.comnet.2017.04.032.

[31] Y. Zhou, X. Zheng, R. Chen, H. Xiong, and S. Guo, "Image-based localization aided indoor pedestrian trajectory estimation using smartphones," *Sensors*, vol. 18, no. 1, p. 258, Jan. 2018, doi: 10.3390/s18010258.

[32] A. Belmonte-Hernández, G. Hernández-Peñaloza, F. Álvarez, and G. Conti, "Adaptive fingerprinting in multi-sensor fusion for accurate indoor tracking," *IEEE Sensors J.*, vol. 17, no. 15, pp. 4983–4998, Aug. 2017, doi: 10.1109/JSEN.2017.2715978.

[33] X. Li, D. Wei, Q. Lai, Y. Xu, and H. Yuan, "Smartphone-based integrated PDR/GPS/Bluetooth pedestrian location," *Adv. Space Res.*, vol. 59, no. 3, pp. 877–887, Feb. 2017, doi: 10.1016/j.asr.2016.09.010.

[34] W. Zhao, S. Han, R. Q. Hu, W. Meng, and Z. Jia, "Crowdsourcing and multisource fusion-based fingerprint sensing in smartphone localization," *IEEE Sensors J.*, vol. 18, no. 8, pp. 3236–3247, Apr. 2018, doi: 10.1109/JSEN.2018.2805335.

[35] N. Oudjane and C. Musso, "Progressive correction for regularized particle filters," in *Proc. 3rd Int. Conf. Inf. Fusion*, Paris, France, Jul. 2000, pp. THB2/10–THB2/17. [Online]. Available: https://ieeexplore.ieee.org/stamp/stamp.jsp?tp=&arnumber=859873

[36] J. D. Hobby and M. Dashti, "A method to incorporate floor plan constraints into indoor location tracking: A Voronoi approach," *Mobile Inf. Syst.*, vol. 2018, Dec. 2018, Art. no. 5303616, doi: 10.1155/2018/5303616.

[37] M. S. Lee, H. Ju, and C. G. Park, "Map assisted PDR/Wi-Fi fusion for indoor positioning using smartphone," *Int. J. Control, Automat. Syst.*, vol. 15, no. 2, pp. 627–639, Apr. 2017, doi: 10.1007/s12555-015-0342-2.

[38] L.-K. Liu and E. Feig, "A block-based gradient descent search algorithm for block motion estimation in video coding," *IEEE Trans. Circuits Syst. Video Technol.*, vol. 6, no. 4, pp. 419–422, Aug. 1996, doi: 10.1109/76.510936.

[39] C. Gao and R. Harle, "Semi-automated signal surveying using smartphones and floorplans," *IEEE Trans. Mobile Comput.*, vol. 17, no. 8, pp. 1952–1965, Aug. 2018, doi: 10.1109/TMC.2017.2776128.

JINGQI FU received the B.Sc. degree from the Northeast Heavy Machinery Institute, in 1984, the M.Sc. degree from Yanshan University, in 1989, and the Ph.D. degree from the Nanjing University of Science and Technology, in 1995. He is currently a Professor with Shanghai University. His current research interests include network measurement and control technology.

AOLEI YANG received the B.Sc. degree from the Hubei University of Technology, Hubei, China, in 2004, the M.Sc. degree from Shanghai University, Shanghai, China, in 2009, and the Ph.D. degree from Queen's University Belfast, Belfast, U.K., in 2012.

From 2013 to 2016, he was a Lecturer with Shanghai University, where he has been an Associate Professor with the School of Mechatronic Engineering and Automation, since 2016. His current research interests include wireless networked control systems, machine learning and computer vision, cooperative control of multiagents, and formation flight control of unmanned aerial vehicles.

ANG LI received the B.Sc. degree from Shanghai University, Shanghai, China, in 2013, where she is currently pursuing the Ph.D. degree in control science and engineering. Her research interests include positioning in wireless network, algorithm optimization, and neuro-engineering.

HUAMING SHEN received the B.Sc. and M.Sc. degrees from Shanghai University, where he is currently pursuing the Ph.D. degree in control science and engineering. His primary research interest includes optimal control theory.

● ● ●